BROOKHAVEN
NATIONAL LABORATORY

BNL-77018-2006-CP

# *Effects of material improvement on CZT detectors*

Muren Chu[a], S. Terterian[a], D. Ting[a], G.A. Carini[b], G.S. Camarda[b], A.E. Bolotnikov[b], R.B. James[b], Dan Xu[c], and Zhong He[c]

[a]Fermionics Corporation, 4555 Runway St, Simi Valley, CA 91362
[b]Brookhaven National Lab, P.O. Box 5000, Upton, NY 11973
[c]Nuclear Engineering and Radiological Science Department, U. of Michigan, Ann Arbor, MI 48109

*Presented at the SPIE, Hard X-ray and Gamma-Ray Detectors Physics VIII*
*San Diego, California*
*August 14th, 2006*

**Nonproliferation and National Security Department**
**Detector Development and Testing Division**

**Brookhaven National Laboratory**
P.O. Box 5000
Upton, NY 11973-5000
www.bnl.gov

# DISCLAIMER

# Effects of material improvement on CZT detectors

Muren Chu*, S. Terterian, D. Ting, G.A. Carini[a], G.S. Camarda[a], A.E. Bolotnikov[a], R.B. James[a], Dan Xu[b], and Zhong He[b]

Fermionics Corporation, 4555 Runway St, Simi Valley, CA 91362
[a]Brookhaven National Lab, P.O. Box 5000, Upton, NY 11973
[b]Nuclear Engineering and Radiological Science Department, U. of Michigan, Ann Arbor, MI 48109

## ABSTRACT

CZT material quality improvement has been achieved by optimizing the crystal growth process. N-type conductivity has been measured on as-grown, undoped $Cd_{0.9}Zn_{0.1}Te$. $Cd_{0.85}Zn_{0.15}Te$ crystals have been grown for producing high resistivity CZT radiation detectors. The best FWHM of $^{57}$Co 122KeV spectrum was measured to be 3.7% and $(\mu\tau)_e$ was $3x10^{-3}$ $cm^2V^{-1}$. The microscopic gamma ray response using a beam size of 10μm has been used to map the entire 4 mm x 4 mm detector. Several black spots indicating no signal responses were observed while all other areas showed an average of 65-70% collection efficiency. The black spots suggest that at those locations, the Te precipitates are larger than 10μm. Detailed microscopic infrared transmission measurement on the sample found that most Te precipitates have sizes of 4-6μm. Theoretical analysis of the results suggests that singly and doubly ionized $Te_{Cd}V_{Cd}^2$ might be the shallow and deep donors previously assigned to $Te_{Cd}$ by us.

**Keywords:** CZT, radiation detector, crystal growth, Te precipitates, Te antisites, HgCdTe, infrared detector arrays

## 1. INTRODUCTION

After half-a-century of study, CZT/CdTe gamma ray detectors are finally used for room temperature applications. Among them, the most significant is eV Product's large quantity of discrete detectors for NASA's Gamma Ray Burst observation.[1] Other achievements can be summarized in the papers presented at the IEEE Conference on Nuclear Science, Medical Imaging and Workshop on Room-Temperature Semiconductor X-ray and Gamma-Ray Detectors.[2] University of Michigan has developed techniques to characterize the 3D and depth sensing of CZT detectors.[3,4] Fisk University demonstrated the importance of processing in securing the quality of the CZT detectors.[5] P.N. Luke demonstrated the feasibility of producing high resolution CZT detectors for sensing high energy gamma-ray and particles.[6] Washington State University has advanced research on defects in CZT.[7] Others, including the groups at Pacific Northwest National Laboratory and Los Alamos National Laboratory, all have significant contribution to the development of CZT detectors.[8]

However, the CZT detector production yield is still low and the performances of these detectors are still below our expectation. Some of the factors limiting the performance of CZT detectors were discussed by A.E. Bolotnikov et al.[9] The problem, in our opinion, is the lack of thorough understanding of the defects in CZT/CdTe. Therefore, it is difficult to design a technique to systematically improve the CZT/CdTe quality.

In principle, the best semiconductor detector material needs to have no/low charge trapping defects/impurities and to have sufficient deep level either due to impurity or defect to pin the Fermi level near the center of the bandgap. Our results show that the problem of CZT crystals and detectors is the high density of charge trapping defects. In the last five years, we found that the major defects in CZT/CdTe are Cd vacancies ($V_{Cd}$) and Te antisites ($Te_{Cd}$, Te at Cd sites).[10-14] These two defects behave quite differently. $V_{Cd}$ moves very rapidly and can be generated and annihilated easily. $Te_{Cd}$, on the other hand, cannot diffuse. When they move, they disappear by forming defect complexes such as Te precipitates or dislocations. To make the situation worse, $V_{Cd}$ and $Te_{Cd}$ can merge together to form defect complexes of $Te_{Cd}$·$V_{Cd}$ and $Te_{Cd}$·$V_{Cd}^2$, which are all donors. In addition, $V_{Cd}$ can merge together to form Te inclusions in various sizes. From these discussions, it becomes clear why CZT/CdTe material is so difficult to engineer to reach desired quality.

CZT gamma ray detector research is a by-product of our HgCdTe infrared Focal Plane Array (FPA) development. CZT with 4% Zn has been used as substrates of the liquid phase epitaxial growth of the HgCdTe layers. The performance of the HgCdTe FPAs critically depends on the CZT quality. The same growth parameters have been used for producing CZT gamma ray detectors with higher Zn composition. In 2003-2004, a modified growth process was developed to grow CZT (4% Zn) for producing high yield HgCdTe arrays. Afterwards, the same parameters have been applied for growing CZT gamma ray detectors. This paper presents our CZT gamma ray results using the new process.

## 2. ELECTRICAL PROPERTIES OF CZT

Table 1 summarizes the general electrical properties of 11,300 CZT/CdTe crystals produced at Fermionics from 1980-2006. Before 1995, all as-grown, undoped crystals were p-type, similar to what everyone else has claimed. Unfortunately, those materials have very high densities of defects, defect complexes, and Te precipitates. A typical example is that the p-type materials always have a low infrared transmission of 63% or less comparing to a theoretical 67% (33% reflection loss). The reduced transmission is a sign of Te precipitates. In 1995, we developed a scheme to reduce the densities of defects in CdTe and $Cd_{0.96}Zn_{0.04}Te$ and the as-grown material became n-type. The infrared transmission of the n-type materials is always higher than 65%, a sign of low defect density.

Table 1. Evolution of electrical properties of CdTe/CZT produced at Fermionics

| Technology of | Parameters | X (Zn Contents) (As-grown, Undoped CZT) | | | |
|---|---|---|---|---|---|
| | | 0.0 | 0.04 | 0.07 | 0.10 |
| 1980-1995 | Conduction Type | P | P | | |
| 1995-2003 | Conduction Type | N | N | | |
| March 2000 | Conduction Type | N | N | N or P | P |
| | Carrier Density at 300K | $1\text{-}5 \times 10^{14}$ | $2\text{-}4 \times 10^{14}$ | - | $4\text{-}6 \times 10^{14}$ |
| November 2003 | Conduction Type | | N | | N |
| | Carrier Density at 300K | | $1\text{-}10 \times 10^{15}$ | | $3 \times 10^{10}$ |

In March 2000, Fermionics started to produce $Cd_{0.9}Zn_{0.1}Te$ and found that the as-grown material is actually p-type in contrast to the n-type conduction of CdTe and $Cd_{.96}Zn_{0.04}Te$.[10] After the studies of the effects of excess Te on the $Cd_{0.9}Zn_{0.1}Te$[11] and the effects of Zn on CZT,[12] we developed a detailed qualitative model to explain the defect dynamics.[12] In November 2003, based on this model, we developed another technique to reduce the generation of defect complexes and Te precipitates. As a result, the as-grown $Cd_{0.9}Zn_{0.1}Te$ became n-type.

## 3. EFFECTS OF CZT QUALITY ON HgCdTe MATERIALS AND ARRAYS

Our qualification standards for $Cd_{.96}Zn_{0.04}Te$ are (i) high infrared transmission (63% or higher) and (ii) n-type resistivity and our specifications for LongWave HgCdTe (wavelength longer than 10 µm) epilayers are (i) high electron mobility and (ii) medium undoped electron concentration ($1 \times 10^{15}$ $cm^{-2}V^{-1}s^{-1}$), and low diode leakage current. The yield data of our $Cd_{.96}Zn_{0.04}Te$ as far as CZT resistivity and HgCdTe electron mobility are concerned is shown in Tables 2 and 3. The crystals in Table 2 were produced in summer 2004 and those in Table 3 were grown after one more year of advancement of the growth process. The improvement of the resistivity control from Table 2 to Table 3 can be clearly observed. Most crystals in Table 3 have a very narrow resistivity range of 1-14 Ω·cm.

Because of the excellent CZT substrates, we were able to produce state-of-the-art HgCdTe focal plane arrays. Fig. 1 shows an imaging picture taken by a 320x256 HgCdTe focal plane array camera with a wavelength of 13.8µm at 85K. This is the longest wavelength ever achieved at this temperature. We definitely attribute this result to the success in CZT substrate quality advancement. Using the high quality CZT substrate, we were also able to deliver 80 units of 128x128 LWIR FPAs to Lockheed Martin in 2005.

Table 2. CZT (4% Zn) grown in summer 2004.

| CZT | Optical Transmission @ 3000 | Conduction Type | Resistivity | Electron Mobility of LWIR HgCdTe Grown on the CZT |
|---|---|---|---|---|
| 10834-R-B4 | 62-65% | N | H (High) | 101,000 (A-) |
| 10835-R-D3 | 61-62% | N | H | 120,000 (A) |
| 10849-R-D3 | 63-65% | N | 20 | 150,000 (A) |
| 10851-N-A3 | 62% | P | 600 | 120,000 (A) |
| 10855-N-E4 | 63% | N | 70 | 130,000 (A) |
| 10856-N-E2 | 62-64% | N | 30 | 120,000 (A) |
| 10857-N-A4 | 65% | N | 29K | 112,000 (A-) |
| 10859-N-B4 | 64% | N | H | 97,000 (B+) |
| 10862-N-E2 | 63-65% | N | H | 70,000 (B-) |
| 10863-N-A3 | 63-65% | N | H | 118,000 (A-) |
| 10864-N-D4 | 65-66% | N | H | 115,000 (A-) |
| 10866-N-B1 | 63-65% | N | 46 | 108,000 (A-) |
| 10867-N-D3 | 62% | N | 1.8M | 120,000 (A) |
| 10876-R-E4 | 63-65% | N | 120 | 50,000 (B-) |
| 10878-R-E2 | 64-65% | N | 10 | 97,000 (B+) |
| 10879-R-D4 | 65-66% | N | H | 120,000 (A) |
| 10881-R-B1 | 64-65% | N | 0.76 | 102,000 (A-) |
| 10882-R-A4 | 64-65% | N | 0.9 | 160,000 (A+) |

Table 3. CZT (4% Zn) grown in spring 2005.

| CZT | Optical Transmission | Conduction Type | Resistivity (Ω·cm) |
|---|---|---|---|
| 11028-N-D4 | 63-66% | N | 1.4 |
| 11030-N-A3 | 64-65% | N | 13.9 |
| 11043-N-A3 | 64-66% | N | 2.6 |
| 11049-N-D3 | 63-66% | N | 9.1 |
| 11051-N-E4 | 63-65% | N | 8.4 |
| 11054-N-D4 | 63-66% | N | 4.2 |
| 11055-N-A3 | 63-66% | N | 2.3 |
| 11056-N-B1 | 62-64% | N | 12.5 |
| 11057-N-A3 | 62-65% | N | 2.0 |
| 11060-N-E1 | 63-66% | N | 5.0 |
| 11066-N-E4 | 64% | N | 1.8 |
| 11069-R-B2 | 64% | N | 8.8 |
| 11070-N-E2 | 64-65% | N | 113K |
| 11074-R-B3 | 64-65% | N | H |
| 11081-R-B1 | 64-66% | N | 21K |
| 11083-N-A4 | 63-66% | N | 3.6 |
| 11085-N-A4 | 62-65% | N | 5.2 |
| 11086-N-B1 | 63-65% | N | 30 |

Fig. 1. Imaging picture taken by a 320x256 HgCdTe FPA with a cutoff wavelength of 13.75μm at 85K.

## 4. PROPERTIES OF GAMMA RAY DETECTORS PRODUCED BY THE NEW CZT PROCESS

The process used to produce CZT in Table 3 was employed to grow CZT crystals for gamma ray detectors. Since (1) the undoped $Cd_{0.9}Zn_{0.1}Te$ are now n-type as shown in Table 1 and (2) its easier to use indium to compensate holes to achieve high resistivity, we decided to work on $Cd_{0.85}Zn_{0.15}Te$ instead of $Cd_{0.9}Zn_{0.1}Te$.

### 4.1 Growth parameters for high-resolution CZT crystals

Table 4 lists the CZT crystals grown with the parameters that generate best resolutions, uniformity, and reproducibility. The Zn composition in these crystals is 15%. The amount of excess Te is either 1.25% or 1.5%. For 1.25% excess Te, $5.0x10^{-4}$ grams of indium is sufficient for CZT to reach high resistivity while for 1.5% excess Te, $6.5x10^{-4}$ grams of indium is required. Under these conditions, the top 65% of the CZT crystals are p-type with high resistivity while the lower 35% are n-type with lower resistivity. The Cd and Zn source materials were purchased from Honeywell while Te was from China.

Table 4. Parameters for Producing High Resolution CZT Detectors.

| 15% Zn CZT w/ Excess Te of | | Crystal Diameter | Indium | Resistivity (Ω·cm) | | FWHM Co57 122keV | |
|---|---|---|---|---|---|---|---|
| 1.25% | 1.5% | | | Center | Top | Center | Top |
| 10815 | | 1.5" | 5.0E-4 | 1E10 | 6E9 | 5.5% | 4.0% |
| 10974 | | 1.5" | 5.1E-4 | 2E7 (N) | 1E10 | - | 5.5% |
| 11022 | | 1.5" | 5.0E-4 | 1E10 | 6E9 | 5.1% | 3.7% |
| | 10830 | 1.5" | 6.6E-4 | 1E10 | 5E9 | 4.7% | 5.0% |
| | 10831 | 1.5" | 5.5E-4 | 4E9 | 8E9 | 5.1% | 4.8% |
| | 10955 | 1.5" | 6.6E-4 | Saw Damage | | | |
| | 10975 | 1.5" | 6.5E-4 | 6E9 | 1E10 | 5.4% | 4.7% |
| | 11068 | 1.5" | 6.5E-4 | 5E9 | 1E10 | 5.3% | 5.0% |

Detectors in sizes of 4mmx4mmx3mm to 5mmx5mmx3mm were fabricated on the above crystals and the FWHM of $^{57}Co$ 122 keV spectra are listed in Table 4. In average, there is no considerable difference between the CZT grown with 1.25% and with 1.5% excess Te. Fig. 2 shows the best $^{57}Co$ 122keV resolution of 3.7%, which was measured on detectors from CZT 11022. Fig. 3 is the spectrum of a detector from CZT 10831, showing a resolution of 4.8%. Crystals with faster or slower post-growth cooling rates have also been grown and analyzed, but their qualities were inferior.

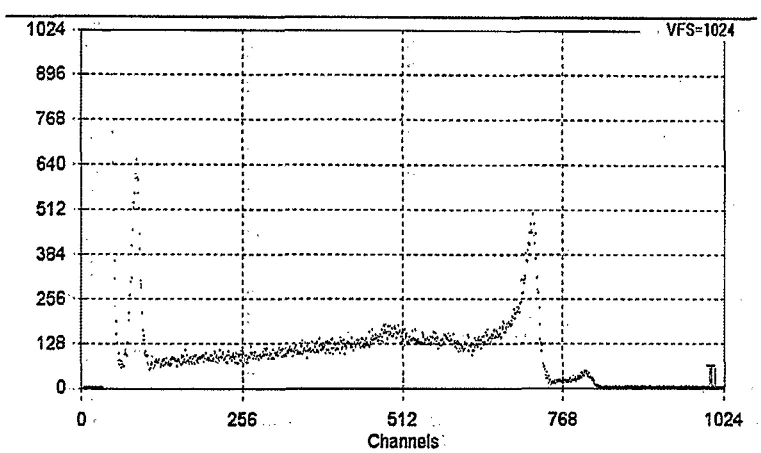


Fig. 2. Detectors from CZT 11022 have a very high $^{57}Co$ 122keV resolution of 3.7%

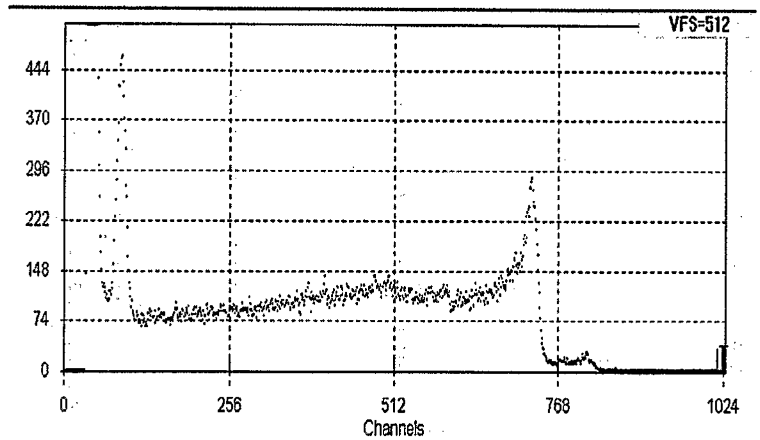


Fig. 3. Detectors from CZT 10831 have a $^{57}$Co 122keV resolution of 4.8%.

### 4.2 Effects of Te precipitates on CZT detectors

One of the detectors fabricated on CZT10815 was delivered to Brookhaven National Laboratory (BNL) for evaluations. The first experiment was the mapping of gamma ray response across the 4mmx4mm detector using a gamma ray beam in a size of 10µmx10µm. The overall mapping result is shown on the left side of Fig. 4. Some contours displaying the variation of the response are observed. The overall response efficiency is from 58-70%. The marked portion of the detector-mapping picture is magnified and presented on the right side of Fig. 4. Several black spots in the gamma ray beam size of 10µmx10µm are revealed. It was postulated that Te precipitates in sizes of 10µmx10µm or larger totally blocked the electrons and holes generated by the gamma ray and allowed no signal to be collected.

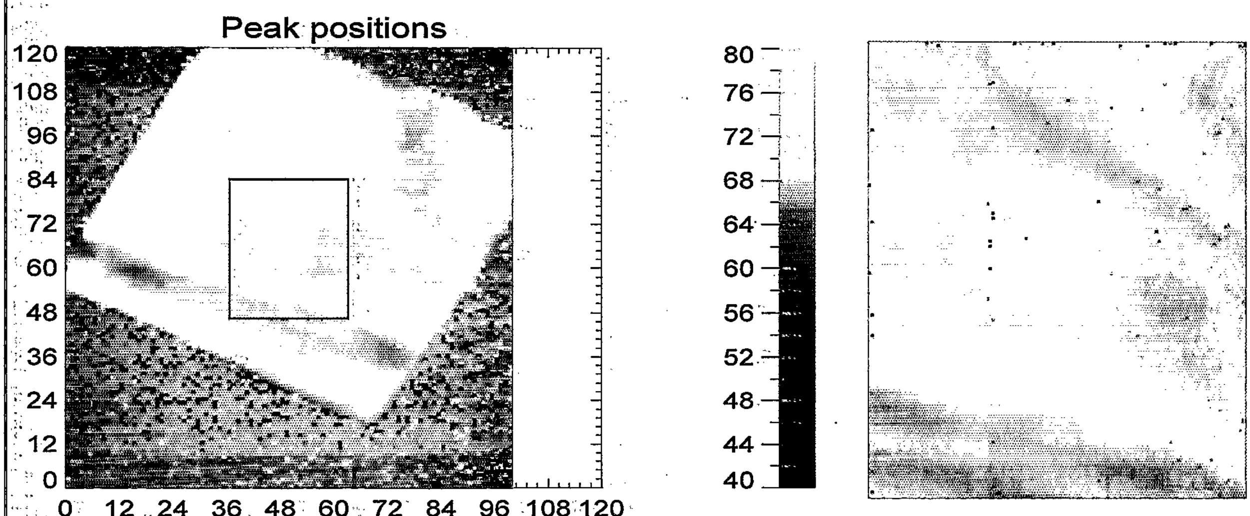


Fig. 4. (Left) The mapping of gamma ray response on a 4mmx4mm CZT detector using a gamma ray beam size of 10µmx10µm and (right) magnified picture showing some 10µm size black spots.

To verify the above hypothesis, infrared mapping was conducted on the sample at BNL. The overall result is displayed on the left side of Fig.5. The stepping size is 0.4mmx0.5mm. The marked unit is amplified and presented on the right side of Fig. 5. Some Te precipitates with large one in sizes of 4-7µm are visible. The lack of Te precipitates larger than 10µm in size is consistent with Fig. 4 results that few black spots were found.

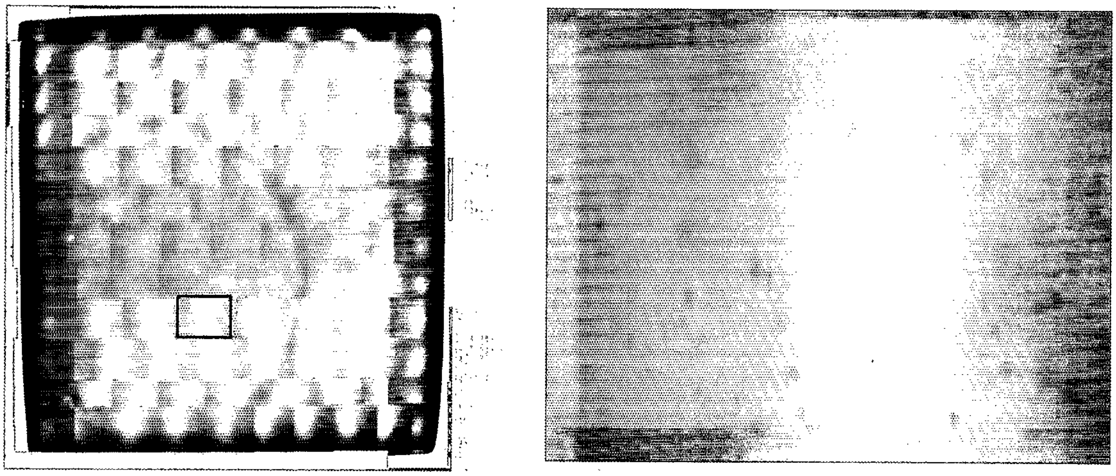

Fig. 5. (Left) The mapping of infrared transmission on the detector in Fig. 4 and (right) the magnified picture of the 0.4mmx0.5mm unit shows some Te precipitates with large ones in sizes of 4-7μm.

### 4.3 1cm x 1cm x 1cm CZT detectors

Two 1cm x 1cm x 1cm CZT detectors, one from CZT 10815 and one from CZT 10831 were fabricated. Picture of the packaged detector is shown in Fig. 6. Surrounded with a guard ring, the large detector size is 1cm x 1cm. In the center of the 1cm x 1cm detector, there were four small 1mm x 1mm pixel anodes. Both units were shipped to Prof. Zhong He at University of Michigan for evaluation.

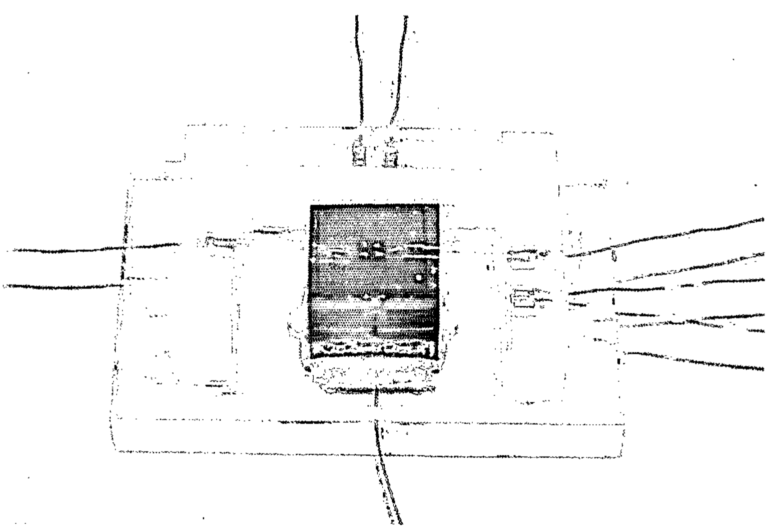

Figure 6. Mounted 1 cm x 1cm x 1cm CZT detector.

Detailed analyses were carried out on the two detectors. In Table 5, we only list the resistivity and $(\mu\tau)_e$ for discussion. The breakdown voltage of the large detector from CZT 10815 is –700V, indicating some surface leakage current. Consequently, the resistivity is low. On the small pixels, there was no surface leakage current and the resistivities were measured to be $1.4\text{-}1.8\times10^{10}$ Ω·cm. The $(\mu\tau)_e$ of this detector, measured by two methods are $3.2\times10^{-3} - 4.2\times10^{-3}$ $cm^2V^{-1}$. The second detector was fabricated from CZT 10831. The surface leakage current is absorbed by the guard ring, which allows the large detector to be biased to more than –1000V. There is not much variation of the resistivity among the large detector and the small ones, all in the range of $1.9\text{-}2.4\times10^{10}$ $cm^2V^{-1}$. The $(\mu\tau)_e$ of this detector is $2.4\times10^{-3}$ $cm^2V^{-1}$.

Table 5. Testing results on 1cmx1cmx1cm detectors

| Crystal | Parameter | Guard Ring | Large Detector | Small Pixel | | | |
|---|---|---|---|---|---|---|---|
| | | | | 1 | 2 | 3 | 4 |
| CZT 10815* (1.25% Ex. Te) | Resistivity (Ω·cm) | | 4.3E9 | 1.6E10 | 1.4E10 | 1.5E10 | 1.8E10 |
| | Breakdown Voltage | | -700V | | | | |
| | $\mu_e\tau_e$ ($cm^2V^{-1}$) | | $3.2x10^{-3} - 4.2x10^{-3}$ | | | | |
| CZT 10831** (1.5% Ex. Te) | Resistivity (Ω·cm) | 2.49E9 | 1.9E10 | 1.9E10 | 2.4E10 | 1.9E10 | 2.3E10 |
| | Breakdown Voltage | | -1000V | | | | |
| | $\mu_e\tau_e$ ($cm^2V^{-1}$) | | $2.4x10^{-3}$ | | | | |

* Ineffective guard ring or surface leakage effect
** 5% charge sharing between small pixels

### 4.4 Comparison with earlier results

Comparison of the new results with those previously published is listed in Table 6. Either 1.25% or 1.5% excess Te was added to the growth melts for the growth of the 15% Zn CZT crystals. The best $^{57}$Co 122keV resolution for this work is 3.7% comparing to 5.5% achieved earlier. The medium $^{57}$Co 122keV resolution in this work is 4.8% comparing to 7% reported before. Besides the much-improved resolution, the uniformity of the detector grade material in each boule is improved from 20% o 50%. The location of the 20% uniformity in previously reported 10%Zn CZT actually changes place from boule to boule. The current reproducibility is also very good. Eighty percent of the boules grown under the same conditions show similar characteristics

Table 6: Comparison of the new results with those previously published.

| | Before Year 2003 | Year 2005 |
|---|---|---|
| Zn Composition | 10% | 15% |
| Excess Te | 1.5% | 1.25% and 1.5% |
| Furnace Profile | Year 1997 Parameter | Adjusted |
| CZT Diameter | 1.5" | 1.5" |
| Best $^{122}$Co FWHM | 5.5% | 3.7% |
| Average $^{122}$Co FWHM | 7% | 4.8% |
| Detector Uniformity | 20% | Over 50% |
| Reproducibility | Detector Uniformity Region Varies from Boule to Boule | 80% |

## 5. THEORETICAL ANALYSIS AND DEFECT MODEL

During the same period we were conducting our research in 1998 to 2002, Wei and Zhang were also performing theoretical calculation on defects in CdTe using first-principles band structure methods.[15] Some of the interesting results are shown in Fig. 7. The 0.1 eV donor level is now assigned to Cd antisite ($Cd_{Te}$) instead of the generally accepted Cd interstitial ($Cd_i$). The $Cd_i$ level is now calculated to be 0.45 eV. Related to our work are the two $Te_{Cd}$ levels, which were calculated to be 0.34 and 0.59 eV. These two data are contradicting to the two levels we assigned to $Te_{Cd}$ in Ref 10. This controversy needs to be addressed.

In our brief discussion with Dr. Wei, the chief scientist at National Renewable Energy Laboratory about the controversy of the donor levels of Te antisites, we mentioned that the shallow donor level is real on every sample and it must be related to $Te_{Cd}$ even if it's not $Te_{Cd}$. Then in 2003 IEEE Conference on Room Temperature Semiconductor X-ray and Gamma-Ray Detectors in Portland, Lynn[16] presented the donor levels of $V_{Cd}$·$Te_{Cd}$ and $V_{Cd}$·$Te_{Cd}^2$ calculated by Dr. Wei. The most interesting data is that the singly ionized $V_{Cd}$·$Te_{Cd}^2$ has an energy level in the conduction band. This is very close to our measured 0.01 eV donor level, which we assigned to $Te_{Cd}^+$ in Ref. 10. Another data is that the doubly ionized energy level of $V_{Cd}$·$Te_{Cd}^2$ is near the center of CdTe bandgap. This level is very close to the deep level considered by Fiederle[17] to be the level of the $Te_{Cd}^+$ and later was considered to be $Te_{Cd}^{++}$ by us.[10] If Wei's calculation is correct, our model in Ref. 10 can be modified by changing $Te_{Cd}$ to $V_{Cd}$·$Te_{Cd}^2$. The rest of the model is still correct.

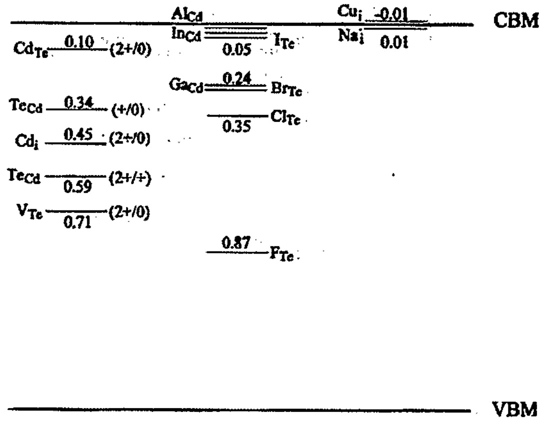


Fig. 7. Calculated donor transition energy levels in CdTe.[15]

Because of the above arguments, we always pay attention to the origin of the shallow level and the deep level. So far, we found that for both 10%Zn CZT and 15% Zn CZT, 1.5% excess Te gives us better resistivity uniformity than those with less amount of excess Te. This fact let us believe that for reaching high resistivity, both Te antisites and Cd vacancies are required. Therefore, the two levels assigned to $Te_{Cd}$ in Ref.10 might very well be $Te_{Cd}V_{Cd}^2$. In this case, Wei's calculation that $Te_{Cd}$ have relatively deep levels might be correct. More experiments are needed to verify this postulation.

## 6. SUMMARY

CZT material quality improvement has been achieved by optimizing the crystal growth process. N-type conductivity has been measured on as-grown, undoped $Cd_{0.9}Zn_{0.1}Te$. $Cd_{0.85}Zn_{0.15}Te$ crystals have been grown for producing high resistivity CZT radiation detectors. The best FWHM of $^{57}$Co 122KeV spectrum was measured to be 3.7% and $(\mu\tau)_e$ was $3\times10^{-3}$ $cm^2V^{-1}$. The microscopic gamma ray response using beam size of 10μm has been used to map the entire 4 mm x 4 mm detector. Several black spots indicating no signal responses were observed while all other areas showed an average of 65-70% collection efficiency. The black spots suggest that at those locations, the Te precipitates are larger than 10μm. Detailed microscopic infrared transmission measurement on the sample found that most Te precipitates have sizes 4-6μm. Theoretical analysis of the results suggests that singly and doubly ionized $Te_{Cd}V_{Cd}^2$ might be the shallow and deep donors previously assigned to $Te_{Cd}$ by us.

## REFERENCES

1. Csaba Szeles, The 2002 U.S. Workshop on the Physics and Chemistry of II-VI Materials, San Diego.
2. Ralph James, General Chair of 2003 IEEE Conference on Nuclear Science, Medical Imaging and Workshop on Room-Temperature Semiconductor X-ray and Gamma-Ray Detectors, Portland, 2003.
3. E. Zhang, Z. He, G.F. Knoll, D.K. Wehe, J.E. Berry, D. Xu, IEEE 13th International Workshop on Room-Temperature Semiconductor X-ray and Gamma-Ray Detectors, Portland, 2003.
4. Z. He, IEEE 13th International Workshop on Room-Temperature Semiconductor X-ray and Gamma-Ray Detectors, Portland, 2003.
5. A. Burger, IEEE 13th International Workshop on Room-Temperature Semiconductor X-ray and Gamma-Ray Detectors, Portland, 2003.
6. P.N. Luke, IEEE 13th International Workshop on Room-Temperature Semiconductor X-ray and Gamma-Ray Detectors, Portland, 2003.
7. K.G. Lynn, IEEE 13th International Workshop on Room-Temperature Semiconductor X-ray and Gamma-Ray Detectors, Portland, 2003.

8. C.E Aalseth, D.S. Barnett, M. Bliss, W. Mengesha, C. Shawley, Abstract of IEEE 13th International Workshop on Room-Temperature Semiconductor X-ray and Gamma-Ray Detectors, p. 196, Portland, 2003.
9. A.E. Bolotnikov, G. Camarla, G.W. Wright, amd R. B. James, IEEE 13th International Workshop on Room-Temperature Semiconductor X-ray and Gamma-Ray Detectors, Portland, 2003.
10. M. Chu, S. Terterian, D. Ting, S. Mesropian, R.H. Gurgenian, and C.C. Wang, "Tellurium Antisites in CdZnTe," Appl. Phys. Lett. 79, 2728 (2001).
11. M. Chu, S. Terterian, D. Ting, C.C. Wang, R.B. James, and A. Burger, "Effects of Excess Tellurium on CdZnTe Detectors," J. of Electron Mater. 32, 778 (2003).
12. M. Chu, S. Terterian, and D. Ting, "Role of Zn in CZT Radiation Detectors," IEEE NSS/MIC Conference, 2003, Manuscript submitted.
13. S. Terterian, M. Chu, D. Ting, C.C. Wang, M. Szawlowski, G.J. Visser, and Paul Luke, "Uniformity and Reproducibility of CdZnTe Radiation Detectors," J. of Electron Mater., 32, 796 (2003).
14. S. Terterian, M. Chu, and D. Ting, "Distribution of the High Resistivity Region in CdZnTe and it Effects on Gamma-ray Detector Performance," Accepted for publication by J. Electron.Mater.
15. S.-H. Wei and S.B. Zhang, Phys. Rev. B 66, 155221 (2002).
16. K.G. Lynn, IEEE 13th International Workshop on Room-Temperature Semiconductor X-ray and Gamma-Ray Detectors, Portland, 2003 (unpublished).
17. M. Fiederle, C. Eiche, M. Salk, R. Schwarz, K.W. Bens, W. Stadler, D.M. Hofmann, and B.K. Meyer, J. Appl. Phys. 84, 6689 (1998).

## Acknowledgement

This work was supported by DOE SBIR Phase I Contract DE-FG02-04ER83955. The contract monitor was David Spears.